Characterization of Protein Immobilization at Silver Surfaces by Near Edge X-ray Absorption Fine Structure Spectroscopy

Xiaosong Liu,[†] Chang-Hyun Jang,[‡,#] Fan Zheng,[†] Astrid Jürgensen,[§] J. D. Denlinger,[||] Kimberly A. Dickson,[¶] Ronald T. Raines,[¶,^] Nicholas L. Abbott,[‡] and F. J. Himpsel*,[†]

Departments of Physics, Chemical and Biological Engineering, Biochemistry, and Chemistry, University of Wisconsin-Madison, Madison, Wisconsin 53706

Received April 11, 2006. In Final Form: June 21, 2006

Ribonuclease A (RNase A) is immobilized on silver surfaces in oriented and random form via self-assembled monolayers (SAMs) of alkanethiols. The immobilization process is characterized step-by-step using chemically selective near-edge X-ray absorption fine structure spectroscopy (NEXAFS) at the C, N, and S K-edges. Causes of imperfect immobilization are pinpointed, such as oxidation and partial desorption of the alkanethiol SAMs and incomplete coverage. The orientation of the protein layer manifests itself in an 18% polarization dependence of the NEXAFS signal from the N 1s to π^* transition of the peptide bond, which is not seen for a random orientation. The S 1s to C−S σ^* transition exhibits an even larger polarization dependence of 41%, which is reduced to 5% for a random orientation. A quantitative model is developed that explains the sign and magnitude of the polarization dependence at both edges. The results demonstrate that NEXAFS is able to characterize surface reactions during the immobilization of proteins and to provide insight into their orientations on surfaces.

1. Introduction

The translation of protein-based analytical methods from bulk solution to surfaces has the potential to greatly expand and accelerate the scope and rate of biological discovery. In particular, the adsorption of proteins on surfaces in known orientations is important for the preparation of assays and sensors[1−6] and is useful for the study of protein activity.[7,8] Consequently, the development of methods to assess the orientation of proteins on surfaces has been a focus of considerable research activity in recent years.[9−13] By using some newly developed schemes that employ use of self-assembled monolayers (SAM), streptavidin layers, or phospholipid bilayers, it is now possible to achieve site-specific attachment of proteins on surfaces, control the surface density, increase the orientational order, and reduce the denaturation of protein.[10,13−16]

Traditional characterization techniques, such as ellipsometry, attenuated total reflection, quartz microbalance, and fluorescent tagging, are aimed at determining the wet and dry mass uptake upon adsorption of proteins at surfaces.[17] When combined with highly specific antibody reactions, they can provide information about the biochemical activity of a surface. To characterize details of the processes occurring during immobilization of proteins on surfaces, however, it is desirable to obtain an element-specific and bond-specific picture of the chemical reactions that are taking place. Near-edge X-ray absorption fine structure spectroscopy (NEXAFS) can provide such information.[18] It measures optical dipole transitions from core levels to unoccupied valence orbitals. By selecting the transition energy, it is possible to focus on a specific valence orbital, projected onto a specific atom in a well-defined oxidation state.[19] In addition, the orientation of the orbital can be determined by the polarization dependence of the transition intensity using optical-dipole selection rules. For example, a typical s-to-p transition is dipole-allowed if the electric field vector of the incident soft-X-rays is parallel to the axis of the p-orbital. The observed intensity follows a $\cos^2 \delta$ pattern around the excitation beam axis. Finally, a measurement of the absolute intensity makes it possible to determine the coverage, element by element. While NEXAFS has been routinely applied to organic molecules, polymers, and small biomolecules including short sections of DNA,[20−23] its use in the characterization of protein adsorption processes is still in its infancy.[24−28]

* Corresponding author. E-mail: fhimpsel@wisc.edu.
[†] Department of Physics.
[‡] Department of Chemical and Biological Engineering.
[¶] Department of Biochemistry.
[^] Department of Chemistry.
[§] Canadian Synchrotron Radiation Facility, Synchrotron Radiation Center, Stoughton, WI 53589-3097.
[||] Lawrence Berkeley National Laboratory, 1 Cyclotron Rd., Berkeley, CA 94720.
[#] Current address: Korea Electrotechnology Research Institute, South Korea.

(1) Gu, J.; Yam, C. M.; Li, S.; Cai, C. *J. Am. Chem. Soc.* **2004**, *126*, 8098−8099.
(2) Lee, K.-B.; Park, S.-J.; Mirkin, C. A.; Smith, J. C.; Mrksich, M. *Science* **2002**, *295*, 1702−1705.
(3) Pallandre, A.; DeMeersman, B.; Blondeau, F.; Nysten, B.; Jonas, A. M. *J. Am. Chem. Soc.* **2005**, *127*, 4320−4325.
(4) Wade, J. D.; Hojo, K.; Kawasaki, K.; Johns, T. G.; Catimel, B.; Rothacker, J.; Nice, E. C. *Anal. Biochem.* **2006**, *348*, 315−317.
(5) Wang, Z.; Jin, G. *J. Biochem. Biophys. Methods* **2003**, *57*, 203−211.
(6) Gupta, V. K.; Skaife, J. J.; Dubrovsky, T. B.; Abbott, N. L. *Science* **1998**, *279*, 2077−2080.
(7) Zhen, G.; Eggli, V.; Voros, J.; Zammaretti, P.; Textor, M.; Glockshuber, R.; Kuennemann, E. *Langmuir* **2004**, *20*, 10464−10473.
(8) Trammell, S. A.; Spano, A.; Price, R.; Lebedev, N. *Biosens. Bioelectron.* **2006**, *21*, 1023−1028.
(9) Cherniavskaya, O.; Chen, C. J.; Heller, E.; Sun, E.; Provezano, J.; Kam, L.; Hone, J.; Sheetz, M. P.; Wind, S. J. *J. Vac. Sci. Technol., B* **2005**, *23*, 2972−2978.
(10) Edmiston, P. L.; Lee, J. E.; Cheng, S. S.; Saavedra, S. S. *J. Am. Chem. Soc.* **1997**, *119*, 560−570.
(11) Lee, J. E.; Saavedra, S. S. *Langmuir* **1996**, *12*, 4025−4032.
(12) Yeung, C.; Purves, T.; Kloss, A. A.; Kuhl, T. L.; Sligar, S.; Leckband, D. *Langmuir* **1999**, *15*, 6829−6836.
(13) Luk, Y.-Y.; Tingey, M. L.; Dickson, K. A.; Raines, R. T.; Abbott, N. L. *J. Am. Chem. Soc.* **2004**, *126*, 9024−9032.
(14) Du, Y.-Z.; Saavedra, S. S. *Langmuir* **2003**, *19*, 6443−6448.
(15) Edmiston, P. L.; Saavedra, S. S. *J. Am. Chem. Soc.* **1998**, *120*, 1665−1671.
(16) Edmiston, P. L.; Saavedra, S. S. *Biophys. J.* **1998**, *74*, 999−1006.
(17) Kasemo, B. *Surf. Sci.* **2002**, *500*, 656−677.
(18) Stohr, J. *NEXAFS Spectroscopy*; Springer-Verlag: New York, 1996.
(19) Zheng, F.; Perez-Dieste, V.; McChesney, J. L.; Luk, Y.-Y.; Abbott, N. L.; Himpsel, F. J. *Surf. Sci.* **2005**, *587*, 191−196.
(20) Crain, J. N.; Kirakosian, A.; Lin, J. L.; Yuedong, G.; Shah, R. R.; Abbott, N. L.; Himpsel, F. J. *J. Appl. Phys.* **2001**, *90*, 3291−3295.

10.1021/la060988w CCC: $33.50
Published on Web 08/08/2006

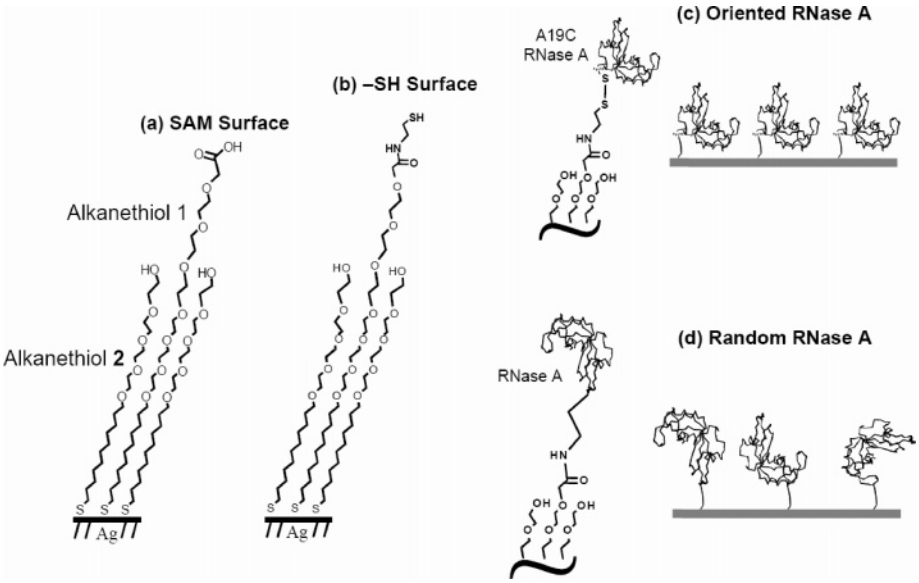

Figure 1. Approach leading to RNase A immobilization on a silver surface investigated by NEXAFS. (a) Mixed SAM of a long chain alkanethiol 1 (for attaching RNase A) and a short chain alkanethiol 2, which serves as a diluent. (b) Alkanethiol SAM with an outer −SH group for immobilizing RNase A with a preferred orientation by method A (see text for details). (c) Oriented RNase A immobilized on surface shown in (b). (d) RNase A immobilized randomly by method B using the surface shown in (a).

This work is intended to explore the capabilities of NEXAFS in a more complex situation, involving a protein, ribonuclease A (RNase A),[29] and multistep immobilization techniques for controlling the bonding and orientation of the protein at a surface.[13] In particular, the orientation effects in NEXAFS have not yet been addressed for molecules as large as RNase A, which contains 951 non-H atoms, 124 amino acids with 123 peptide bonds, and 12 S atoms. At the C edge, we find no detectable polarization dependence due to averaging over the many possible orbital orientations of the 575 C atoms in RNase A. The N edge exhibits a significant polarization dependence of 18%, and the twelve S atoms produce a substantial polarization dependence of 41%. The results are consistent with a quantitative model that averages over all bond orbitals and over random azimuthal orientations. The results demonstrate that orientation measurements are possible for small proteins by using NEXAFS and suggest a strategy for improving their accuracy by utilizing minority elements, such as N, S, and possible substitutional elements at specific sites.

2. Experimental Methods

The substrates used in our study were silver films. Although gold films have been widely used in past studies for immobilization of proteins on thiol-based SAMs, the vicinity of a gold absorption edge near the S 1s edge creates a prohibitive background for the S K-edge measurements. On the other hand, the Ag 3d core level creates a sloping background for the N 1s edge which was removed by comparison with the spectrum of a clean Ag substrate. For the photon yield data, it was sufficient to subtract the spectrum of a clean Ag substrate. The electron yield spectra exhibit a significant attenuation of the Ag substrate and required a more complicated data processing method. They were first divided by the spectrum of a clean silver film evaporated in situ on silicon, and a linear fit to the pre-edge background was subtracted in order to normalize out spectral features of the silver substrate. Then they were divided by a constant factor to normalize the pre-edge background to 1 and obtain a measure of the coverage.

Uniform films of silver with thickness of ∼100 nm were deposited onto silicon wafers by using an electron-beam evaporator. A 5-nm titanium layer was used to promote adhesion between the silicon wafer and the silver film. The substrates were mounted on rotating planetaries during deposition.

The procedures for immobilization of RNase A are described in detail in a previous article.[13] Two immobilization methods were used: one for obtaining oriented adsorption (method A) and the other for random adsorption (method B). Key elements of these approaches, which were characterized by NEXAFS, are shown in Figure 1a−d.

The surface shown in Figure 1a is a mixed SAM of two alkanethiols, 11-[19-carboxymethylhexa(ethylene glycol)]undecyl-1-thiol (**1**), and 11-tetra(ethylene glycol)undecyl-1-thiol (**2**) at a 45:55 mole ratio, deposited on an evaporated silver film. This surface is used in both immobilization methods A and B. The longer chain **1** provides the reaction site for immobilization of RNase A, while the shorter chain **2** serves as the diluent to control the density of immobilized RNase A. The SAM was then activated by EDC/NHS to form a monolayer presenting an NHS ester. For method A, the NHS-activated SAM was transferred to a solution of 20 mM 2-aminoethanethiol and 2 mM diisoproylethylamine for 20 min to form the surface shown in Figure 1b with thiol groups. Oriented immobilization of RNase A was achieved by using a mutant, A19C RNase A, in which residue 19 (alanine) is replaced with a cysteine, activated as a mixed disulfide with 2-nitro-5-thiobenzoic acid (NTB). Immobilization in a preferred orientation was achieved through formation of a disulfide bond between the activated cysteine and a thiol group on the surface. This is depicted in Figure 1c. In method B, wild-type RNase A was directly immobilized on the SAM surface shown in Figure 1a through reaction of the lysine residues and N-terminus in the RNase A to the NHS-activated SAM. There are

(21) Luk, Y.-Y.; Abbott, N. L.; Crain, J. N.; Himpsel, F. J. *J. Chem. Phys.* **2004**, *120*, 10792−10798.
(22) Peters, R. D.; Nealey, P. F.; Crain, J. N.; Himpsel, F. J. *Langmuir* **2002**, *18*, 1250−1256.
(23) Petrovykh, D. Y.; Perez-Dieste, V.; Opdahl, A.; Kimura-Suda, H.; Sullivan, J. M.; Tarlov, M. J.; Himpsel, F. J.; Whitman, L. J. *J. Am. Chem. Soc.* **2006**, *128*, 2−3.
(24) Haralampus Grynaviski, N. M.; Auciello, O.; Carlisle, J. A.; Gerbi, J. E.; Gruen, D. M.; Moore, J. F.; Zinovev, A.; Firestone, M. A. In *Biomicroelectromechanical Systems*; Ozkan, C. S., Santini, J. T., Jr., Gao, H., Bao, G., Eds.; MRS Proceedings 773; Material Research Society: Warrendale, PA, 2003; p 49.
(25) Hitchcock, A. P. *J. Synth. Rad.* **2001**, *8*, 66−71.
(26) Hitchcock, A. P.; Morin, C.; Zhang, X.; Araki, T.; Dynes, J.; Stover, H.; Brash, J.; Lawrence, J. R.; Leppard, G. G. *J. Electron Spectrosc. Relat. Phenom.* **2005**, *144*−*147*, 259−269.
(27) Hitchcock, A. P.; Stover, H. D. H.; Croll, L. M.; Childs, R. E. *Aust. J. Chem.* **2005**, *58*, 423−432.
(28) Ringler, P.; Schulz, G. E. *Science* **2003**, *302*, 106−109.
(29) Raines, R. T. *Chem. Rev.* **1998**, *98*, 1045−1066.

10 lysine residues and an N-terminal amino group presented by each RNase A molecule, such that wild-type RNase A should be immobilized at 11 different sites, resulting in an effectively random orientation. This is depicted in Figure 1d. Detailed procedures for the synthesis of the alkanethiols and the preparation of the A19C RNase A mutant are described by Luk et al.[13] and references therein.

Alkanethiol SAMs have been widely used for chemically or biologically functionalized surfaces because of their stability and order. However, some recent studies[30,31] observe degradation and oxidation, as well as loss of orientational order of the alkanethiol-based SAMs on metal surfaces under biologically relevant conditions (e.g., immersion into PBS buffer[30]) or ambient conditions (e.g., exposure to air and/or light[31]). In our experiments, the SAM shown in Figure 1a was soaked in a solution of EDC/NHS for 40 min and then transferred to a solution of 20 mM of 2-aminoethanethiol and 2 mM of diisopropylethylamine for 20 min to form the −SH surface. These samples were stored in PBS buffer in capped vials for about 2 days. After each step of the preparation procedure, and before being loaded into a vacuum chamber via a load lock, the samples were rinsed with deionized water and dried with a stream of nitrogen. Any or all of these sample preparation steps might have caused partial loss of SAM molecules. Using the intensity of the S 1s NEXAFS signal, we were able to tell whether such a loss occurred and pinpoint the preparation step that caused the loss. This is not possible with standard techniques, such as ellipsometry.

NEXAFS spectroscopy was performed at the C 1s, N 1s, and S 1s edges, both in the total electron yield and the fluorescence yield mode. For the electron yield of the C 1s and N 1s edges, we used the 10-m TGM monochromator at the Synchrotron Radiation Center (SRC) of the University of Wisconsin-Madison. The S 1s edge data in both the electron and fluorescence yield mode were taken at the double crystal monochromator (DCM) of the Canadian Synchrotron Radiation Facility (CSRF)[32,33] at the SRC, using InSb(111) crystals and a nine-element solid-state Ge detector. Fluorescence yield data of the N 1s edge were acquired at Beamline 8.0 of the Advanced Light Source (ALS) in Berkeley using a channel plate with an Al filter. For S 1s measurements, normalization with respect to the incident photon flux was achieved by simultaneous measurement of the TEY of a gas cell containing ~1.5 Torr air and located upstream from the sample. The C 1s and N 1s measurements were normalized to the photocurrent from an upstream Au grid. The photon energy was calibrated at the C 1s edge to the π^* peak of graphite at 285.35 eV (for the SRC data) and at the N 1s edge to the vibrationally resolved π^* peak of molecular N_2 (ALS data),[34] with an accuracy of ±0.2 eV.

To investigate the orientation of the protein molecules, polarization-dependent NEXAFS spectra were collected by using p-polarized light with two incident angles: normal incidence ($\theta = 90°$) and grazing incidence ($\theta = 30°$). Dipole selection rules for transitions from the 1s core levels select final states with p-character. The intensity is maximum when the electric field vector of the light is parallel to the axis of the p-orbital in the final states and falls off with a $\cos^2 \delta$ distribution. For each sample, several spectra were collected at different spots to exclude sample inhomogeneity. In addition, several consecutive scans were performed at the same spot to check for radiation damage of the samples under soft X-ray radiation. No radiation damage was found for up to four consecutive scans at the SRC, while the ALS data had to be restricted to a single scan for each spot, even with a defocused spot and narrow slits. Radiation damage manifested itself by a decrease of the π^* peak of the peptide bond and an additional peak below the peptide π^* peak, which is attributed to a π^* orbital of dehydrogenated C═N configurations.[35,36] These findings are consistent with the photon flux density, which is low enough at the SRC to keep the number of absorbed photons small compared to the number of molecules in the exposed spot.[19]

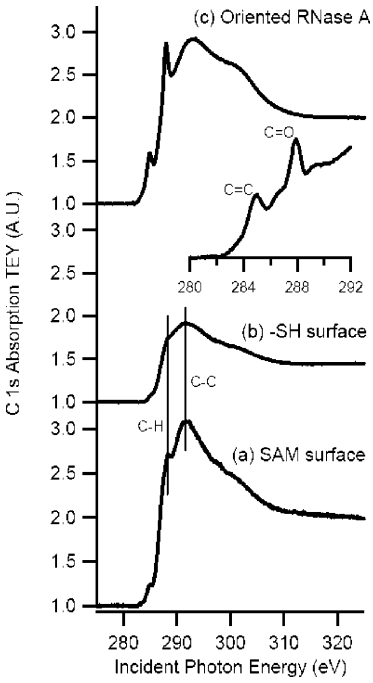

Figure 2. C 1s NEXAFS spectra at normal incidence for three stages of the immobilization of oriented RNase A on silver. (a) Alkanethiol SAM shown in Figure 1a. (b) −SH terminated SAM shown in Figure 1b. (c) Oriented RNase A depicted in Figure 1c. The inset expands the region of the sharp π^* orbitals in (c). The decrease of the C1s NEXAFS intensity between (a) and (b) demonstrates a partial loss of the SAM (even though the S 1s intensity in Figure 4 increases due to the addition of the −SH group). There is no detectable polarization dependence, which reflects the averaging effect over the bond orbitals of 575 C atoms.

3. Results and Discussion

3.1. Carbon 1s Spectra. Figure 2 shows the C 1s NEXAFS spectra for the three steps of the immobilization sequence leading to oriented RNase A, taken at normal incidence ($\theta = 90°$). The spectra were normalized to the pre-edge background from the substrate, which allows a semiquantitative determination of the coverage from the spectral intensity. The integrated C 1s absorption intensity of the −SH surface (Figure 1b) is reduced by a factor of 2 compared to the intensity of original SAM (Figure 1a). It recovers after immobilization of RNase A (Figure 1c). The reduction of the carbon signal indicates a substantial loss of alkanethiols when preparing the surface shown in Figure 1b from the surface shown in Figure 1a, which might be due to sample preparation steps and rinsing procedures. Another reason for the partial loss of the SAM could be the storage of the samples in PBS buffer for 2 days before characterization. The increase of the carbon signal after attachment of RNase A on the −SH surface is an indicator for successful immobilization of protein molecules. These observations are supported by the S 1s results described below.

Next, we focus on the transitions observed in the C 1s NEXAFS spectra. In spectra (a) and (b) of Figure 2, two peaks are observed

(30) Flynn, N. T.; Tran, T. N. T.; Cima, M. J.; Langer, R. *Langmuir* **2003**, *19*, 10909−10915.
(31) Willey, T. M.; Vance, A. L.; Van Buuren, T.; Bostedt, C.; Terminello, L. J.; Fadley, C. S. *Surf. Sci.* **2005**, *576*, 188−196.
(32) Kravtsova, A. N.; Stekhin, I. E.; Soldatov, A. V.; Liu, X.; Fleet, M. E. *Phys. Rev. B* **2004**, *69*, 134109.
(33) Yang, B. X.; Middleton, F. H.; Olsson, B. G.; Bancroft, G. M.; Chen, J. M.; Sham, T. K.; Tan, K.; Wallace, D. J. *Rev. Sci. Instrum.* **1992**, *63*, 1355−1358.
(34) Chen, C. T.; Ma, Y.; Sette, F. *Phys. Rev. A* **1989**, *40*, 6737−6740.
(35) Zubavichus, Y.; Fuchs, O.; Weinhardt, L.; Heske, C.; Umbach, E.; Denlinger, J. D.; Grunze, M. *Radiat. Res.* **2004**, *161*, 346−358.
(36) Zubavichus, Y.; Zharnikov, M.; Shaporenko, A.; Fuchs, O.; Weinhardt, L.; Heske, C.; Umbach, E.; Denlinger, J. D.; Grunze, M. *J. Phys. Chem. A* **2004**, *108*, 4557−4565.

at 288.4 and 292.1 eV. These peaks are assigned to excitations from the C 1s level to σ^* orbitals of C−H and C−C bonds, respectively.[20,37] Weak features at 285.0 eV are assigned to π^* orbitals of π-bonded hydrocarbon contamination on the surfaces. Oriented RNase A in Figure 2c exhibits two sharp π^* orbital peaks at 285.0 and 288.0 eV, which are characteristic of C═C and C═O double bonds, respectively. This energy region is enlarged as the inset in Figure 2. The spectrum of RNase A is similar to an NEXAFS measurement of a bacterial surface layer[38,39] and of some small peptides.[40−42] A comprehensive theoretical and experimental study of the inner shell absorption spectra of all 20 amino acids[43] allows us to interpret the spectra of a protein in terms of its constituent amino acids. The C═C peak at 285.0 eV corresponds to transitions to π^* orbitals located on the side group of amino acids with aromatic rings, such as tyrosine (Tyr) and phenylalanine (Phe). The C═O peak at 288.0 eV can be compared with data from solid glycine (Gly),[41] where it lies 0.4 eV higher. A similar shift is observed in simple peptides Gly-Gly and Gly-Gly-Gly and in fibrinogen,[41] where it is explained by the change from an isolated carboxyl group in glycine to a carboxyl and amide combination in peptides and proteins. An additional shoulder is found on the low-energy side of the C═O π^* peak, at about 287 eV. Vyalikh et al.[38] assign this shoulder to a C═N π^* orbital. This feature is also found in the NEXAFS spectra of AF51 and PPOD,[44] where it was assigned to the C═N π^* orbital of the oxadiazole ring. Judging from a comparison to the NEXAFS spectra of individual amino acids,[43] this shoulder could be due to the side chains of some amino acid residues such as imidazole group in histidine (His) and mercapto group in cysteine (Cys).

A polarization dependence of the NEXAFS signal is not detectable at the C 1s edge. Essentially, the averaging over the bond orbitals of 575 carbon atoms randomizes polarization effects. Highly oriented C1s transitions have been observed in silk protein fibers.[45] These are dominated by repetitions of the [Gly-Ala-Gly-Ala-Gly-Ser]$_n$ hexapeptide sequence, which adopts the antiparallel β-sheet conformation. RNase A does not contain such a highly repetitive sequence. Its β-sheet contributes only 46% of the amino acids, and it is not periodic. The C1s edge is randomized further by the proximity of transitions into different orbitals (see the previous paragraph). For example, the C 1s → π^* transition of the peptide bond cannot be separated from the C 1s → π^*_{COOH} transitions, which lie ∼0.3 eV higher.[40,41] The latter occur in amino acid residues, such as Asp (HOOC−CH_2–CH(NH_2)−COOH) and Glu (HOOC−(CH_2)$_2$−CH(NH_2)−COOH).

3.2. Nitrogen 1s Spectra. Figure 3 shows the N 1s NEXAFS spectra of RNase A immobilized as shown in Figure 1c and 1d.

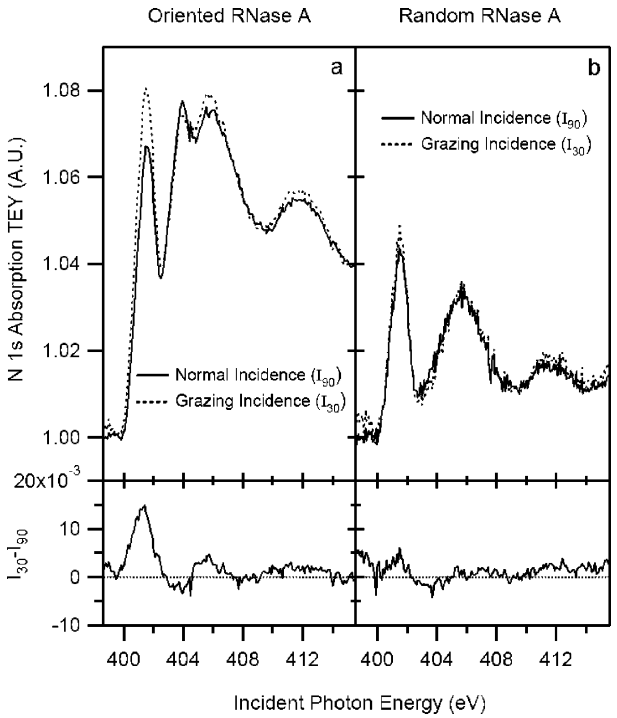

Figure 3. N 1s NEXAFS spectra of oriented RNase A (left) and random RNase (right), as shown in Figure 1c and Figure 1d, respectively. (Samples (a) and (b) do not contain detectable amounts of nitrogen.) The spectrum of sample (c) exhibits a significant polarization dependence of the π^* orbital at 401.5 eV, which is associated with the peptide bond. This is brought out by a difference spectrum in the lower panel. The NEXAFS intensity shows that oriented RNase A exhibits a 50% higher coverage. It also exhibits an extra peak at 403.9 eV, which is assigned to a remnant of the NO_2 group from the protection agent.

Analogous N 1s spectra of the two SAMs shown in Figure 1a and 1b do not exhibit any of the features in Figure 3, confirming that the N 1s spectra are characteristic of the protein molecules. The normalized nitrogen signal from the single layer of RNase A is about 6% with oriented immobilization and 4% with random orientation (at normal incidence). These values are comparable to the nitrogen signal from DNA oligomers.[20] The data in Figure 3 are for the electron yield. The fluorescence yield (acquired at the ALS) gave similar results, for both the polarization dependence and the intensity ratio between oriented and random RNase A (not shown). Only the signal-to-background ratio is improved by a factor of 6.

The N 1s spectra of both RNase A films show a dominant peak at 401.5 eV. It is assigned to the π^* orbital that is delocalized over the O═C−NH group. This peak is also observed in glycine-based oligopeptides (Gly-Gly and Gly-Gly-Gly)[40,41] and Fibrinogen.[41] The absence of this peak in molecular glycine supports this conclusion, because there is no nitrogen next to the O═C group. The C−N peptide bond connects two amino acids. The region of the σ^* orbitals shows a peak at ∼405.4 eV, which is assigned to a combination of and transitions from 1s to N−C and N−H orbitals.[41] A high-lying peak at ∼411.0 eV is attributed to N 1s → $\sigma^*_{C-NH_2}$, σ^*_{C-NH}, and σ^*_{CONH} transitions by comparison to the previous studies of glycine-based oligopeptides.[41]

An extra peak is observed at 403.9 eV in oriented RNase A. This peak is assigned to a remnant of the NO_2 group in the NTB, which was used to protect RNase A variant A19C,[13] staying on the sample surface after immobilization of RNase A. The energy position is close to the transition into the π^* orbital of the NO_2

(37) Kondoh, H.; Nambu, A.; Ehara, Y.; Matsui, F.; Yokoyama, T.; Ohta, T. *J. Phys. Chem. B* **2004**, *108*, 12946−12954.
(38) Vyalikh, D. V.; Danzenbacher, S.; Mertig, M.; Kirchner, A.; Pompe, W.; Dedkov, Y. S.; Molodtsov, S. L. *Phys. Rev. Lett.* **2004**, *93*, 238103.
(39) Vyalikh, D. V.; Kirchner, A.; Danzenbacher, S.; Dedkov, Y. S.; Kade, A.; Mertig, M.; Molodtsov, S. L. *J. Phys. Chem. B* **2005**, *109*, 18620−18627.
(40) Cooper, G.; Gordon, M.; Tulumello, D.; Turci, C.; Kaznatcheev, K.; Hitchcock, A. P. *J. Electron Spectrosc. Relat. Phenom.* **2004**, *137*−*140*, 795−799.
(41) Gordon, M. L.; Cooper, G.; Morin, C.; Araki, T.; Turci, C. C.; Kaznatcheev, K.; Hitchcock, A. P. *J. Phys. Chem. A* **2003**, *107*, 6144−6159.
(42) Zubavichus, Y.; Zharnikov, M.; Schaporenko, A.; Grunze, M. *J. Electron Spectrosc. Relat. Phenom.* **2004**, *134*, 25−33.
(43) Kaznacheyev, K.; Osanna, A.; Jacobsen, C.; Plashkevych, O.; Vahtras, O.; Agren, H.; Carravetta, V.; Hitchcock, A. P. *J. Phys. Chem. A* **2002**, *106*, 3153−3168.
(44) Giebler, R.; Schulz, B.; Reiche, J.; Brehmer, L.; Wuehn, M.; Woell, C.; Smith, A. P.; Urquhart, S. G.; Ade, H. W.; Unger, W. E. S. *Langmuir* **1999**, *15*, 1291−1298.
(45) Hernandez Cruz, D.; Rousseau, M.-E.; West, M. M.; Pezolet, M.; Hitchcock, A. P. *Biomacromolecules* **2006**, *7*, 836−843.

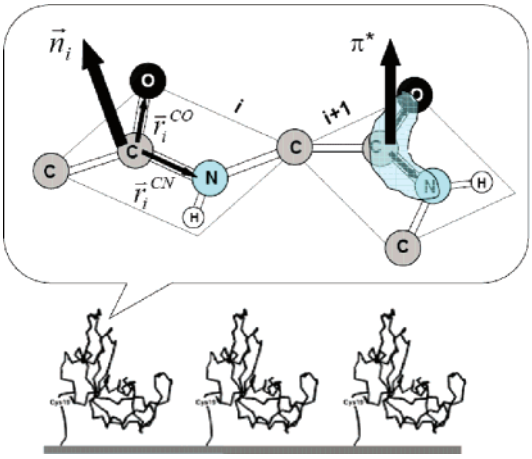

Figure 4. Geometry of the peptide bond. A delocalized π^* orbital extends over the O−C−N bonds (right). The corresponding p-orbital is oriented perpendicular to the plane of peptide bond (arrow).

group (403.5−404.5 eV).[44,46,47] For random immobilization, the wild-type RNase A was attached on the surface. There is no NO_2 group contaminating the surface, and the extra peak is absent.

To evaluate the angular dependence, the spectra for various θ were normalized to a common step height of the N 1s absorption edge (from the pre-edge at 398 eV to the post-edge at 415 eV). Thereby, the spectra become proportional to the absorption per N atom. Difference spectra between grazing and normal incidence are plotted in the bottom panels of Figure 3. The oriented RNase A (Figure 1c) shows a significant polarization dependence of the dominant peak. This observation is consistent with the orientation of liquid crystals found in a previous study.[13] The polarization dependence of the randomly oriented RNase A, on the other hand, is close to the noise level.

3.3. Calculation of the Polarization Dependence for the π^* Orbitals of the Peptide Bonds. The π^* resonances can be described in a molecular orbital picture as dipole transitions from s initial states to the p component of the π^* final states. The NEXAFS intensity I for the transition from an initial state $|i\rangle$ to a final state $|f\rangle$ is given by the optical dipole matrix element:[18]

$$I \propto |\vec{e}\cdot\langle f|\vec{p}|i\rangle|^2 \propto \cos^2\delta \qquad (1)$$

where $\vec{e}$ is the unit vector in the direction of the electric field vector, $\vec{p}$ is the momentum operator, and δ is the angle between the electric field vector and the direction of the final state molecular orbital.

In a protein molecule, amino acids are linked by peptide bonds (Figure 4). The bond electrons are delocalized across the entire peptide bond, and both the carbon−oxygen and the carbon−nitrogen bonds possess double-bond character. Due to the shared π^* orbital, peptide C−N bonds are unable to rotate freely, and the six atoms surrounding a peptide group lie in a single plane.[48] The π^* orbital is oriented perpendicular to the peptide plane, such that:

$$\vec{n}_i = \frac{\vec{r}_i^{\,CO} \times \vec{r}_i^{\,CN}}{|\vec{r}_i^{\,CO} \times \vec{r}_i^{\,CN}|} \qquad (2)$$

where $\vec{n}_i$ is the unit vector along the direction of π^* orbital of ith peptide group, and $\vec{r}_i^{CO}$ and $\vec{r}_i^{CN}$ are the vectors of C−O and C−N bonds of ith peptide group, respectively (Figure 4).

To estimate the combined polarization dependence of all peptide bonds in RNase A, we utilize the structure determined by X-ray crystallography.[49] The vectors $\vec{r}_i^{CO}$ and $\vec{r}_i^{CN}$ are first calculated from the coordinates of the C, N, and O atoms of each peptide bond. Then, the unit vector $\vec{n}_i$ associated with the corresponding π^* orbital is calculated using eq 2. For each individual peptide bond, $I_i(\theta)$ is calculated as a function of X-ray incidence angle θ by eq 3

$$I_i(\theta) = \cos^2\delta_i = (\vec{E}_i\cdot\vec{n}_i)^2 \qquad (3)$$

Finally, the total intensity is calculated by adding all individual $I_i(\theta)$:

$$I(\theta) = \sum_{i=1}^{N} I_i(\theta) \qquad (4)$$

where N is the total number of peptide bonds (N = 123 for RNase A).

For modeling the N 1s data from Figure 3a we assume that all molecules are bound to the supporting SAM via a S−S bond to the cysteine at the 19th residue, and that this S−S bond is perpendicular to the surface (as in Figure 1). Their azimuthal orientation around the S−S bond is assumed to be random, since the substrate is isotropic when averaged over the beam area. The atomic coordinates from the X-ray database are first rotated to align the S−S bond normal to the surface. Then the polarization dependence is calculated for 100 azimuthal rotation angles (from 0 to 2π) around the surface normal. The result is plotted in the top panel of Figure 5 (line) together with the two data points at 90° and 30°, with the 90° point normalized to 1 (normal incidence).

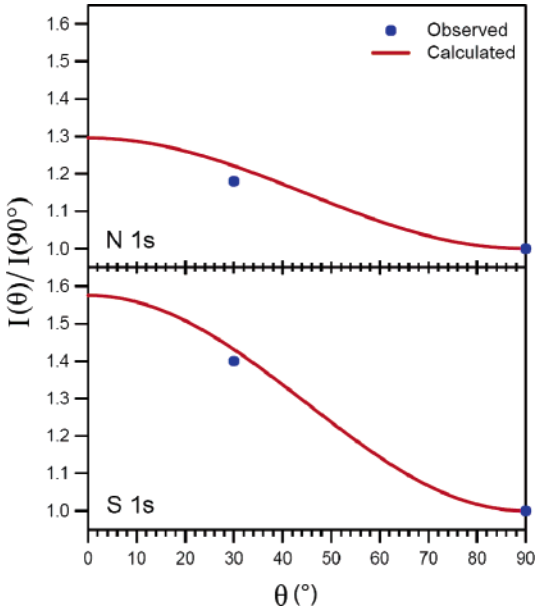

Figure 5. Polarization dependence of the NEXAFS intensity for the transitions from N 1s to the π^* orbital of the peptide bonds (top, from Figure 3a) and from S 1s to the σ^* orbital of the C−S bonds (bottom, from Figure 6c). The model calculation gives the correct sign and magnitude for both transitions, showing that even a molecule with 124 amino acids and 951 atoms (excluding H) is able to produce a significant orientation signal in NEXAFS.

(46) La, Y.-H.; Jung, Y. J.; Kang, T.-H.; Ihm, K.; Kim, K.-J.; Kim, B.; Park, J. W. *Langmuir* **2003**, *19*, 9984−9987.
(47) Petravic, M.; Deenapanray, P. N. K.; Coleman, V. A.; Jagadish, C.; Kim, K. J.; Kim, B.; Koike, K.; Sasa, S.; Inoue, M.; Yano, M. *Surf. Sci.* **2006**, *600*, 81−85.
(48) Nelson, D. L.; Cox, M. *Lehninger Principles of Biochemistry*, 4th ed.; Freeman: New York, 2005.
(49) Liu, Y.; Hart, P. J.; Schlunegger, M. P.; Eisenberg, D. *Proc. Natl. Acad. Sci. U.S.A.* **1998**, *95*, 3437−3442.

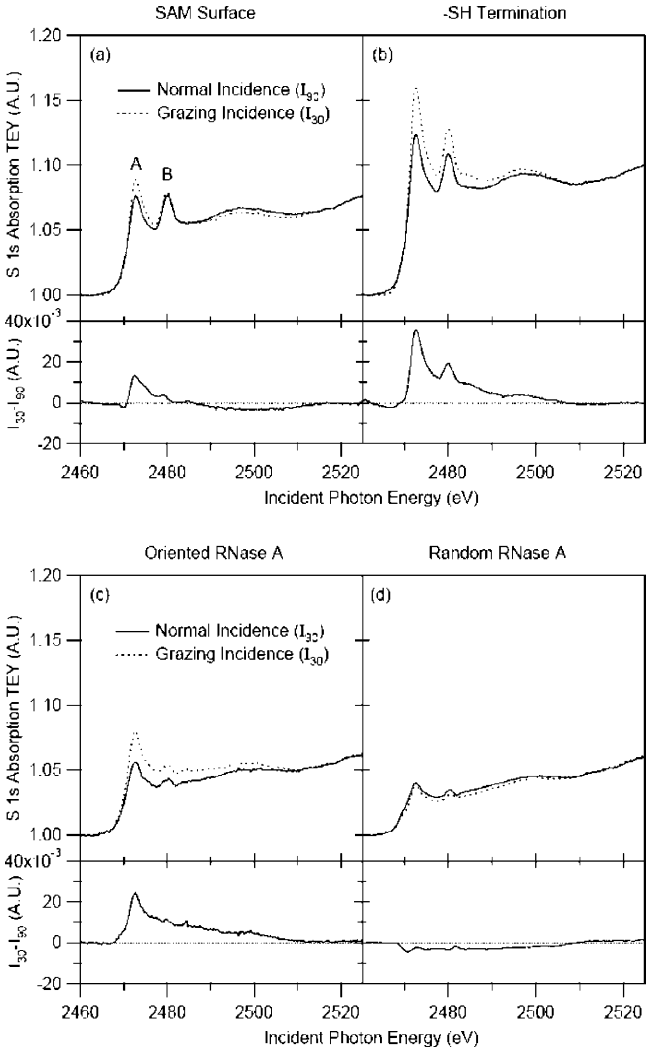

Figure 6. S 1s NEXAFS spectra of all stages of protein immobilization shown in Figure 1. Difference spectra between normal and grazing incidence at the bottom of each panel detect the orientation. Peak A is assigned to the S−C σ* orbital, Peak B to oxidized S.

The experimental modulation between 30° and 90° is 18% for N 1s compared to a calculated modulation of 22%. The signs are correct, and the magnitudes are comparable for both N, which provides an independent test of the method. The results show that the polarization dependence of NEXAFS from this rather complicated molecule can be understood quantitatively.

The fact that the modulation is slightly reduced in the data can be attributed to imperfect polarization of the synchrotron light (93%) and to a small spread in the polar angle of the protein−substrate bond. An additional factor might be partial denaturing of the protein in a vacuum. In our experience, the polarization dependence is stable for a few hours in a vacuum but degrades overnight, which might be due to a loss of the more strongly bound hydration water.

The fairly strong polarization dependence of the peptide bonds is surprising at first. One might think that averaging over 123 bonds would randomize the NEXAFS signal. However, RNase A contains highly correlated regions, such as 22% α-helices and 46% β-sheets, which amplify the polarization dependence. An even stronger polarization dependence is observed for the S bonds, because there are only 12 S atoms in RNase A (see below). That leads to less averaging. This strategy can be generalized: For determining the orientation of a protein, the orbitals of minority species are most useful. Specific markers, such as the substitutional heavy elements used for phasing in protein crystallography, would be rather useful for accurate orientational information from NEXAFS. With more markers the configuration of a protein at a surface can be pinpointed more accurately.

3.4. Sulfur 1s Spectra. Figure 6a−d shows the S 1s NEXAFS spectra of the four surfaces depicted in Figure 1. Similar to the N 1s edge, the spectra were first normalized to a clean silver substrate. A linear fit to the pre-edge background was then subtracted. Similar to the polarization-dependent N 1s spectra in Figure 3, the S 1s spectra in Figure 6 were normalized to a common step height of the S 1s absorption edge (from the pre-edge at 2460 eV to the post-edge at 2520 eV) for all θ.

All S 1s spectra show two clear peaks at 2473 and 2481 eV (peaks A and B). These two peaks have been observed in many sulfur-containing molecules[50−53] and amino acids[54] on metal surfaces. Peak A is assigned to transition of the S 1s electron to the S−C σ* orbital and to transitions within atomic S on the surface. Peak B is assigned to S 1s electron to the σ* orbital of the S−O bond, which is due to an oxidized sulfur species. The formation of the atomic sulfur and oxidized sulfur was demonstrated to result from the scission of the S−C bond in alkanethiol chains, and photooxidation for the sulfur.[52]

From the C edge spectra, we observe that the integrated signal of the surface shown in Figure 1b is reduced compared to the SAM shown in Figure 1a and that it recovers after immobilization of RNase A with method A. We propose that this phenomenon is due to the decomposition and partial removal of the SAMs. This conclusion is supported by previous studies. Lewis et al.[55] found that UV radiation in air of alkanethiol SAM on silver substrate caused the photochemically induced S−C bond scission, desorption of alkyl chain fragments, and oxidation of surface-bound sulfur. Hutt et al.[52] also showed that for octanethiol SAMs on silver, 70 min of photooxidation resulted in all the alkylthiolates being oxidized to alkylsulfonates. Therefore, the decomposition and oxidation of SAMs may be the predominant reasons for the reduction of intensities of absorption signals.

The S 1s signal (both the peaks and step height) increases upon transforming the SAM shown in Figure 1a to that in Figure 1b, contrary to the C 1s edge. This can be explained as the result of the presence of thiol groups from 2-aminoethanethiol coupling with NHS-activated SAMs (refer to Figure 1) on the surface. The signal from these additional thiol groups compensates for the signal reduction caused by the loss of part of the SAMs. In particular, −SH groups enhance the intensity of Peak A, which corresponds to the transition of the S 1s electron to the S−C σ* orbital. Second, after immobilization of RNase A on the surface in either a preferred orientation or random orientation, the intensities drop to a level slightly weaker than that of the SAM surface, with the random RNase A weaker than the oriented RNase A. A qualitative analysis suggests that this signal drop results from three effects: (1) the degradation of SAMs during the protein immobilization procedures and sample storage, (2)

(50) Doomes, E. E.; Floriano, P. N.; Tittsworth, R. W.; McCarley, R. L.; Poliakoff, E. D. *J. Phys. Chem. B* **2003**, *107*, 10193−10197.
(51) Fernandez, A.; Espinos, J. P.; Gonzalez-Elipe, A. R.; Kerkar, M.; Thompson, P. B. J.; Ludecke, J.; Scragg, G.; de Carvalho, A. V.; Woodruff, D. P.; Fernandez-Garcia, M.; Conesa, J. C. *J. Phys.: Condens. Matter* **1995**, *7*, 7781−7796.
(52) Hutt, D. A.; Cooper, E.; Leggett, G. J. *Surf. Sci.* **1998**, *397*, 154−163.
(53) Yagi, S.; Nakano, Y.; Ikenaga, E.; Sardar, S. A.; Syed, J. A.; Tanaka, K.; Hashimoto, E.; Taniguchi, M. *Surf. Sci.* **2004**, *566−568*, 746−750.
(54) Yagi, S.; Matsumura, K.; Nakano, Y.; Ikenaga, E.; Sardar, S. A.; Syed, J. A.; Soda, K.; Hashimoto, E.; Tanaka, K.; Taniguchi, M. *Nucl. Instrum. Methods Phys. Res., Sect. B* **2003**, *199*, 244−248.
(55) Lewis, M.; Tarlov, M.; Carron, K. *J. Am. Chem. Soc.* **1995**, *117*, 9574−9575.

the attenuation of the S photoelectrons from the SAMs by the protein layer (RNase A has a molecular diameter 3.8 nm) on top of the SAMs, and (3) the sulfur-containing amino acids in the protein molecules enhance the intensity of the signal. However, effect (3) is not strong enough to compensate for effects (1) and (2), because only 12 of the 124 amino acid residues in RNase A contain sulfur: eight cysteines and four methionines. In addition, as seen in Figure 6, the ratio of Peak A to Peak B for oriented RNase A (panel c) increased dramatically, compared to the SAM surface (panel a). This increase indicates that the presence of protein molecules mainly contributes to the enhancement of the intensity of Peak A (S 1s electron to the σ^* S−C orbital), as expected from pure protein spectra. The weaker signal from (d) random RNase A is due to the absence of thiol groups during the random immobilization and lower binding ability of the randomly oriented RNase A on the surface, which is consistent with the N 1s spectra (Figure 3).

As shown in Figure 5 (bottom panel) and Figure 6, the intensity modulation from normal incidence (90°) to grazing incidence (30°) provides information about the orientation of molecules on each sample surface. For the S 1s edge, the vector $\vec{r}_i^{SC}$ represents the σ^* orbital of the ith S−C bond in RNase A. It is calculated from the coordinates of the C and S atoms in each sulfur-containing amino acid residue and then normalized to become the vector $\vec{n}_i$ in eq 3. The intensity for each individual bond is calculated by eq 3. In one RNase A molecule, there are 16 S−C bonds (eight from eight cysteines, and eight from four methionines). The experimental modulation between 30° and 90° is 41% for S 1s, compared to a calculated modulation (see above for details) of 44% for the sample depicted in Figure 1c. This sample exhibits the largest polarization dependence, in agreement with the chemical preparation method and the N 1s spectra (Figure 3). Likewise, the polarization dependence is weakest for the sample depicted in Figure 1d. The modulation between 30° and 90° is 5%. As one can see in Figure 6, the modulation is more dramatic for Peak A than Peak B for all samples except random RNase A. This indicates that the surface-bound, oxidized sulfur is less oriented than the sulfur forming S−C bonds in SAMs and RNase A. For the −SH terminated surface, the orientational order of the SAMs is enhanced judging from the increased modulation of peak A (29% in sample (b) compared to 17% in sample (a)).

4. Summary

In summary, we employ element- and bond-sensitive NEXAFS spectroscopy at the C, N, and S 1s edges to investigate the state of RNase A immobilized on silver via self-assembled monolayers. Element-specific information is obtained about the individual steps of two immobilization schemes. Oxidation or loss of alkanethiol molecules can easily be detected. The orientation of the immobilized protein is detected by the polarization dependence of the NEXAFS intensity.

A polarization dependence is observed for both the N 1s and S 1s spectra, using transitions into the π^* orbital of the peptide bond and the σ^* orbital of the S−C bond, respectively. The C 1s spectra are isotropic, due to the large number of carbon orbitals with different orientations. A quantitative model is developed for calculating the polarization dependence, which explains both the sign and the magnitude of the observed intensity modulation (18% for N 1s and 41% for S 1s). The increased modulation at the S 1s edge is attributed to the fewer number of S atoms in the protein, which reduces the averaging effect. That suggests the utility of minority species for determining the orientation of a protein at a surface. Examples would be substitution of S by Se and other substitutions by heavy elements, which are commonly used for phasing in protein crystallography.

These results suggest that NEXAFS can be used to investigate fairly complex organic molecules immobilized on a surface, such as proteins containing more than 100 amino acid residues. Such element-specific, surface-sensitive diagnostics can facilitate the development of a fuller understanding of processes occurring at interfaces that support proteins.

Acknowledgment. We acknowledge Mark Bissen (SRC) and Anna Kiyanova (Department of Chemical and Biological Engineering, UW-Madison) for help in preparing silver films, Jason Crain (NIST) for getting the experiment started, and Jeet Kalia (Department of Biochemistry, UW-Madison) for providing helpful discussions. This work was supported by the NSF under Awards DMR-0520527 (MRSEC) and DMR-0537588 (SRC) and by the DOE under Contracts No. DE-FG02-01ER45917 and No. DE-AC03-76SF00098 (ALS). N.L.A. thanks the NIH for financial support under R01 CA 108467-01. Financial support for CSRF is provided by the Natural Sciences and Engineering Research Council of Canada (NSERC) and National Research Council Canada-Conseil National de Recherches Canada (NRC-CRNC).

LA060988W